Available online at www.sciencedirect.com
SCIENCE DIRECT®
Microporous and Mesoporous Materials 65 (2003) 197–208
MICROPOROUS AND MESOPOROUS MATERIALS
www.elsevier.com/locate/micromeso

Transport mechanisms of water and organic solvents through microporous silica in the pervaporation of binary liquids

Johan E. ten Elshof *, Cristina Rubio Abadal, Jelena Sekulić, Sankhanilay Roy Chowdhury, Dave H.A. Blank

Inorganic Materials Science group, MESA+ Research Institute and Faculty of Science and Technology, P.O. Box 217, 7500 AE Enschede, The Netherlands

Received 10 June 2003; received in revised form 8 August 2003; accepted 15 August 2003

Abstract

Pervaporation experiments were performed on microporous silica membranes in the temperature range 30–80 °C using binary liquids containing 5–22 wt.% water. The organic solvents used were methanol, *N*,*N*-dimethylformamide (DMF) and 1,4-dioxane. The dependency of flux and selectivity on temperature and feed composition were investigated. The results were interpreted in terms of the Maxwell–Stefan theory, and Maxwell–Stefan diffusion coefficients at 60 °C were estimated. Water, methanol and DMF were found to diffuse through silica by a surface diffusion mechanism, while 1,4-dioxane was transported mainly by viscous flow through mesopores or small defects. DMF inhibited the transport of water, which may be explained by micropore blocking by strongly adsorbed DMF molecules. The flux of methanol appears to be dominated by a dragging effect by the larger water flux.

Keywords: Pervaporation; Membrane; Silica; Maxwell–Stefan; Diffusion

1. Introduction

Pervaporation is a separation process in which a liquid mixture is placed in contact with one side of a membrane, while the other side is kept under vacuum. The transport of components is driven by a chemical potential gradient across the membrane. Separation of components occurs due to selective evaporation and subsequent diffusion of the most volatile and mobile components from the liquid feed. Due to the fact that only a fraction of the liquid feed is vaporized, the energy efficiency is better than competing distillation technology. Pervaporation can be applied for several purposes, e.g., separation of azeotropic mixtures and dehydration during esterification reactions [1]. Using well-known polymeric membranes, pervaporation established itself relatively quickly as a new type of unit operation. However, the applicability of such membranes is limited to temperatures up to ~130 °C, while their performance in terms of flux and selectivity is often limited to a narrow range of solvents and feed concentrations. Zeolite and microporous ceramic membranes exhibit superior thermal, mechanical and chemical stabilities in this respect. Zeolite membranes are known to be very

* Corresponding author. Tel./fax: +31-53-4892695.
E-mail address: j.e.tenelshof@utwente.nl (J.E. ten Elshof).

1387-1811/$ - see front matter © 2003 Elsevier Inc. All rights reserved.
doi:10.1016/j.micromeso.2003.08.010

Nomenclature

c	concentration (mol m^{-3})
Đ	Maxwell–Stefan micropore diffusivity (m^2 s^{-1})
Đ$^{\text{eff}}$	effective diffusion coefficient (m^2 s^{-1})
E^D	activation energy of diffusion (J mol^{-1})
E^F	activation energy of permeability (J mol^{-1})
F	permeability (mol m^{-2} s^{-1} Pa$^{-1)}$
H	adsorption (Henry) coefficient (mol m^{-3} Pa^{-1})
K	Henry coefficient or $1/RT$ (mol m^{-3} Pa^{-1}).
J	flux (mol m^{-2} s^{-1})
L	membrane thickness (m)
p	partial pressure (Pa)
Δp	partial pressure difference (Pa)
Q	heat of adsorption (J mol^{-1})
R	gas constant (J mol^{-1} K^{-1})
T	temperature (K)
v	velocity (m s^{-1})
w	weight fraction
x	mole fraction in adsorbed (membrane) phase
$\bar{x}$	average molar fraction
z	direction of transport (m)

Greek symbols

α	separation factor
μ	chemical potential (J mol^{-1})
μ^0	standard chemical potential (J mol^{-1})

Subscripts

i,j	liquid components type i,j
M	membrane
w	water
s	solvent

Superscripts

f	feed
p	permeate
0	pre-exponential constant

selective because of their well-defined pore structure and size and are particularly useful for dehydration processes in which low water concentrations should be reached. The separation of organic components using zeolites with high Si/Al ratio has also been reported [2–5]. A disadvantage of some zeolites is that due to their ion-exchange nature they may be susceptible to salts and acidic and alkaline media. Ceramic pervaporation membranes are more robust and exhibit high fluxes, although they are often less selective than zeolite and polymer membranes [6].

At present the most mature ceramic membrane for pervaporation is the asymmetric stacked system consisting of a macroporous α-alumina support, a mesoporous γ-alumina intermediate layer and a microporous silica top layer [7–11]. This system is also applicable for gas separation [12,13]. The silica top layer is made by acid-catalyzed sol–gel synthesis and has a narrow pore size distribution with pore sizes between 0.3 and 0.55 nm [14].

The flux and selectivity of pervaporation membranes are usually expressed in terms of total mass flux (kg m^{-2} h^{-1}) and separation factor α [8]. For a binary liquid with components i and j the latter factor is defined as follows:

$$\alpha = \frac{w_i^{\text{p}}/w_j^{\text{p}}}{w_i^{\text{f}}/w_j^{\text{f}}}, \tag{1}$$

where w^{p} and w^{f} refer to the mass fractions of i and j in the permeate and feed (retentate), respectively. Although these parameters provide a good measure of process performance and a qualitative indication of membrane permeability and selectivity, they do not explain the intrinsic differences in pervaporation behavior of different species on the molecular scale. For instance, the value of α depends strongly on the ratio $w_i^{\text{f}}/w_j^{\text{f}}$, which is a process variable that is not related to the nature of the membrane, or the diffusion and adsorption processes that occur.

Various models have been proposed to describe the transport of binary liquids through pervaporation membranes, especially for polymeric ones [15]. Among those, the Maxwell–Stefan theory is based on the thermodynamics of irreversible pro-

cesses, and takes the effect of interactions between the individual mobile components into account explicitly. The Maxwell–Stefan equations regard the steady state transport of a component as a balance between the driving force of that component, and the friction forces exerted by the membrane and the other components. The first application of the Maxwell–Stefan theory to pervaporation was by Heintz and Stephan for polymeric membranes [16]. The theory has been used to describe the pervaporation processes of several polymeric membranes [17,18]. A description of pervaporation through a ceramic microporous membrane in terms of the Maxwell–Stefan equation was given by Verkerk et al. [19]. Unlike the modified Maxwell–Stefan equations for polymeric membranes [16], which consider volume fractions instead of molar fractions, and describe the driving forces in terms of concentration differences across the membrane, they modeled the molecular transport in terms of vapor partial pressure differences and molar fractions, which are more applicable quantities for the description of vapor transport through microporous layers with a fixed pore structure.

In this paper the pervaporation characteristics of three types of 5–20 wt.% water-containing binary liquids based on methanol, *N*,*N*-dimethylformamide and 1,4-dioxane, respectively, through microporous silica membranes are discussed. The aim of the study is to describe the transport behavior of these liquids on molecular scale and to give an explanation for the differences in behavior between liquids with different types of organic components.

2. Theory

Considering the one-dimensional transport of a mobile component i from a binary mixture of components i and j through a membrane M, the driving force of component i can be expressed in terms of the Maxwell Stefan theory by [19]

$$-\frac{1}{RT}\frac{\mathrm{d}\mu_i}{\mathrm{d}z} = \frac{x_j}{Đ_{ij}}(v_i - v_j) + \frac{1}{Đ'_{iM}}v_i, \tag{2}$$

where z is the direction of transport (perpendicular to the membrane surface area), T the temperature, R the gas constant, μ_i the chemical potential of component i, x_j the mole fraction of component j in the adsorbed (membrane) phase, $Đ_{ij}$ the Maxwell–Stefan micropore diffusivity between components i and j, $Đ'_{iM}$ the Maxwell–Stefan micropore diffusivity of component i in the membrane, and v_i and v_j the velocities of components i and j in the membrane, respectively. The first term on the right hand side of Eq. (2) describes the friction on species i caused by the presence of species j, while the second term indicates the friction exerted on species i by the membrane. If correlation effects between i and j can be neglected, $1/Đ_{ij} = 0$.

Under the assumption that the components are transported as individual gaseous species via surface or activated gas-phase diffusion [20], an expression for the driving force can be obtained using the chemical potential of an ideal gas-phase component, i.e.,

$$\mu_i = \mu_i^0 + RT\ln p_i, \tag{3}$$

where μ_i^0 and p_i are the standard chemical potential and partial pressure of component i, respectively. The velocity v_i, in Eq. (2) can be written as the ratio of flux J_i and local concentration c_i, i.e, $v_i = J_i/c_i$, so that

$$-\frac{1}{p_i}\frac{\mathrm{d}p_i}{\mathrm{d}z} = \frac{x_j}{Đ_{ij}}\left(\frac{J_i}{c_i} - \frac{J_j}{c_j}\right) + \frac{1}{Đ'_{iM}}\frac{J_i}{c_i}. \tag{4}$$

The expression for the concentration c_i depends on whether the main mode of transport through the micropores is by gas translation or by surface diffusion. In the former case the molecules inside the micropores retain a gaseous character, although their movement becomes restricted, and has to overcome certain energy barriers imposed by the micropore channels [20]. The local concentration of molecules can be approximated by $c_i = p_i/RT$. The second case, surface diffusion, is a hopping-type mode of transport that includes Langmuir-type adsorption on the internal pore walls. At low levels of adsorption (Henry's law regime), the concentration of a component is proportional to the local vapor pressure in the membrane [12,19], i.e.,

$$c_i = H_i p_i, \tag{5}$$

where H_i is the adsorption coefficient of component i, that depends on temperature according to [12]

$$H_i = H_i^0 \exp(Q_i/RT). \tag{6}$$

Here Q_i is the heat of adsorption of i (>0) and H_i^0 is a pre-exponential constant. It is also possible that the transport of a certain species is partly by surface diffusion, and partly by activated gas diffusion.

For a binary liquid, Eq. (4) indicates a set of two coupled equations that can be solved numerically if the molar fraction x_j is known as a function of position z inside the membrane. The simplifying assumption made here is that x_j can be approximated by the average of the molar fractions on opposite sides of the membrane $\bar{x}_j$ [17].

An explicit expression for J_i can be obtained from Eq. (4) if J_j/c_j is negligible in comparison with J_i/c_i. For a membrane of thickness L the expression for J_i, then reads

$$J_i = K_i \left(\frac{\bar{x}_j}{Đ_{ij}} + \frac{1}{Đ'_{iM}} \right)^{-1} \frac{\Delta p_i}{L}, \tag{7}$$

where $\Delta p_i = p_i^{\mathrm{f}} - p_i^{\mathrm{p}}$, with p_i^{f} and p_i^{p} the vapor partial pressures of component i at the feed and permeate side of the membrane, respectively. The factor K_i is equal to either H_i (pure surface diffusion) or $1/RT$ (pure gas-phase translation). The factor containing the Maxwell–Stefan diffusivities can be regarded as the effective diffusion coefficient $Đ_i^{\mathrm{eff}}$:

$$Đ_i^{\mathrm{eff}} = \left(\frac{\bar{x}_j}{Đ_{ij}} + \frac{1}{Đ'_{iM}} \right)^{-1}. \tag{8}$$

The temperature dependency of $Đ_i^{\mathrm{eff}}$ will be complex, depending on both physical phenomena such as the activation energy of hopping of species along surface adsorption sites and surface coverage, but also on external process variables such as the composition at the feed and permeate sides of the membrane. However, in sufficiently small temperature intervals it maybe approximated by an Arrhenius-type expression

$$Đ_i^{\mathrm{eff}} = Đ_i^{\mathrm{eff},0} \exp(-E_i^D/RT), \tag{9}$$

where E_i^D and $Đ_i^{\mathrm{eff},0}$ are the apparent activation energy of diffusion and a pre-exponential constant, respectively.

From Eqs. (7) and (8) the permeability F_i can be expressed as

$$F_i = \frac{J_i}{\Delta p_i} = \frac{K_i Đ_i^{\mathrm{eff}}}{L}, \tag{10}$$

so that the activation energy of permeability E_i^F is either $E_i^F = E_i^D - Q_i$ (surface diffusion), or $E_i^F \approx E_i^D$ (gas translation).

3. Experimental

Tubular α-alumina supported microporous silica membranes with a γ-alumina intermediate layer between the support and the silica top layer were obtained from Pervatech, the Netherlands. Silica sols were made by acid-catalyzed hydrolysis and condensation of tetra-ethoxy-orthosilicate as described in more detail elsewhere [14]. The silica sols were deposited by a flow coating technique on the inner surface of the tubes, which had an inner diameter of 6.5 mm, and were calcined at ~400 °C. The part of the tubes exposed to the liquid feed in the pervaporation experiments was 0.08 m long (total membrane surface area 16.3 cm^2). The silica layer had a thickness of ~100 nm.

Pervaporation experiments were performed in the temperature range of 30–80 °C. The feed mixtures were binary liquids with 5–22 wt.% water (on total weight) in methanol (Merck, 99.7%), 1,4-dioxane (Riedel, 99.5%) or *N*,*N*-dimethylformamide (DMF, Merck, >99%). Pervaporation experiments with pure liquids were also performed. The feed mixture, contained in a 1 l heated vessel under a pressure of 3.5 bar, was pumped continuously through the feed compartment of the pervaporation unit, where it was stirred and came into direct contact with the silica top layer of the membrane. The pervaporation unit and membrane were kept at the desired temperature using an oil bath. The retentate was recycled to the feed vessel.

The permeate side of the membranes was kept under near-vacuum (8–10 mbar) with a vacuum pump. Steady state fluxes were determined by collecting the permeate side vapors in a dry ice

cold trap and measuring the weight increase with time. The water concentration in the feed was determined by Karl Fischer titration and the permeate composition was determined from the coefficient of refraction. The partial vapor pressures at the feed side was calculated from $p_i^f = x_i\gamma_i p_i^0$, where x_i is the molar fraction of i in the liquid phase, γ_i the activity coefficient, and p_i^0 the vapor pressure of pure i at a given temperature. The values of γ_i were calculated with the Wilson equation, and p_i^0 with the Antoine equation [21]. The partial vapor pressures at the permeate side were calculated from the molar fractions in the permeate and the total pressure.

4. Results and discussion

The total mass fluxes (water + 2nd component) and corresponding separation factors for 15 wt.% water-containing binary liquid feeds at temperatures between 30 and 80 °C are shown in Fig. 1. The influence of water concentration on mass flux and separation factor at 60 °C is shown in Fig. 2. The highest fluxes and separation factors, varying between 1.3–2.5 kg m^{-2} h^{-1} and 120–185 at 60 °C, respectively, were found for the 1,4-dioxane/water mixtures. The high separation factor in this process can be explained qualitatively by the large kinetic diameter of 1,4-dioxane (>0.65 nm) in

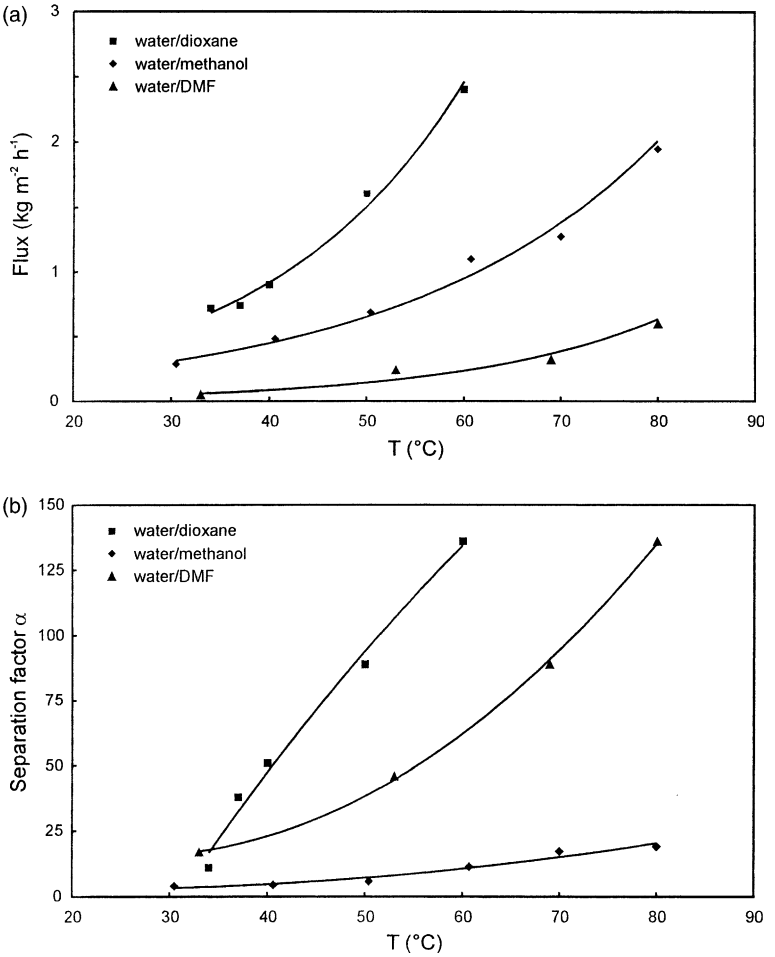

Fig. 1. Temperature dependency of (a) total mass fluxes and (b) separation factors in pervaporation of binary liquids with 15 wt.% water in liquid retentate. Drawn lines in (a) are exponential fits to the experimental data. Drawn lines in (b) are a guide to the eye.

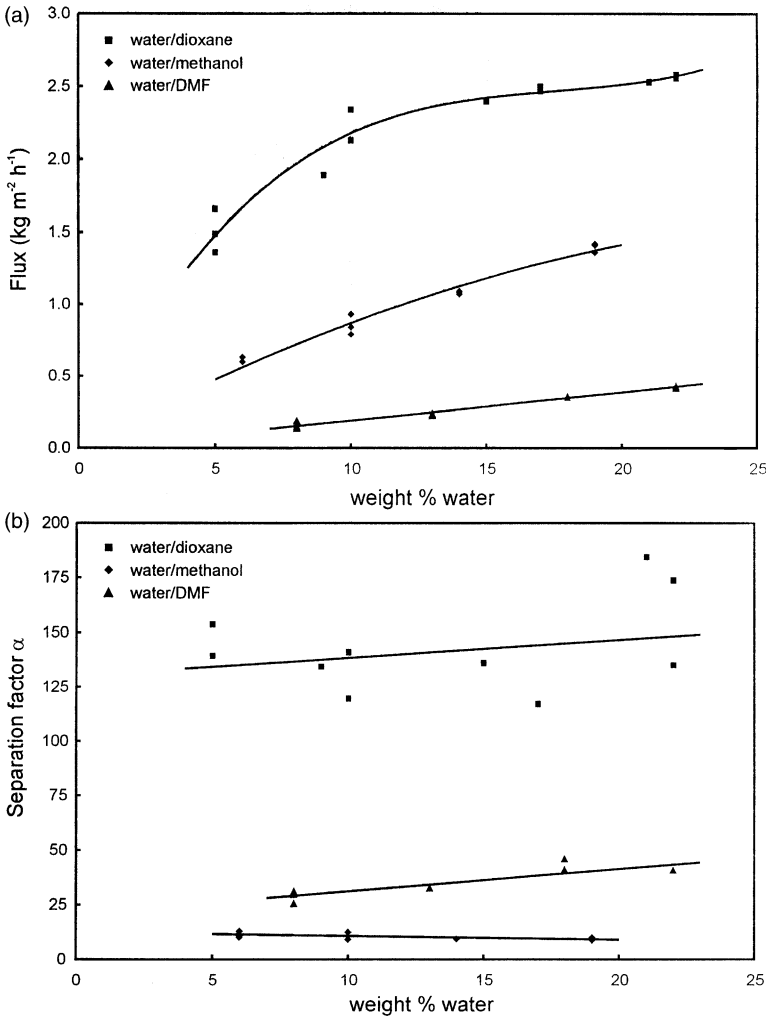

Fig. 2. (a) Total mass fluxes and (b) separation factors in pervaporation of binary liquids at 60 °C versus retentate composition. Drawn lines are a guide to the eye.

comparison with the sizes of the other molecules (see Table 1) and the silica pore size of 0.3–0.55 nm [14]. The aliphatic segments of 1,4-dioxane and its small dipole moment may further complicate the penetration of this molecule into the hydrophilic silica layer and its diffusion through pores.

The low separation factors of 9–13 in the separation of water/methanol can be explained by considering that methanol is only slightly larger than water, while its dipole moment is only a little smaller. Methanol will therefore be able to penetrate the silica pores effectively, and in view of the

Table 1
Solvents and their physical properties[a]

Molecule	Kinetic diameter (nm)	Dipole moment (D)
Water	0.26	1.85
Methanol	0.38–0.41	1.70
DMF	~0.55[b]	3.82
1,4-dioxane	~0.7[b]	0

[a] Data were taken from Refs. [4,22,23] (kinetic diameter) and Ref. [4] (dipole moment).

[b] Kinetic diameters of DMF and 1,4-dioxane were estimated from the diameters of molecules of similar size and chemical nature.

silica pore size a significant fraction of the connecting paths should have a wide enough diameter for methanol to be transported through the layer.

With respect to the separation of DMF/water, a combination of very low fluxes (<0.5 $kg\,m^{-2}\,h^{-1}$) and reasonable separation factors (25–50) at 60 °C was found. DMF is considerably larger than water and methanol, but it also has a very large dipole moment, so that strong attractive interactions between silica and DMF are expected. Shah et al. also observed very low mass fluxes of DMF/water mixtures through hydrophilic zeolite NaA membranes [4]. They attributed the low fluxes to the effect of strong DMF adsorption on the internal zeolite surface, thereby blocking the channels for water transport. The same explanation may hold for the low flux through microporous silica.

This suggests that DMF is small enough to enter the silica pores, but diffuses slowly, so that water transport is hindered substantially.

The apparent activation energies E_{act} of the fluxes calculated from the data of Fig. 1 are listed in Table 2. For all three binary liquids the activation energies for water transport are in the same range, i.e., 45–55 kJ/mol, which is close to the activation energy of ~45 kJ/mol for pervaporation of water through zeolite NaA membranes [4]. The E_{act} values of the fluxes of organic solvents are considerably smaller (<20 kJ/mol). As molar transport occurs by vapor-phase species, the values of E_{act} in Table 2 contain a contribution from the increase of the feed side vapor pressure p_i^f with increasing temperature. The temperature dependency of the permeability $F_i = J_i/\Delta p_i$ provides a better measure to compare the thermally activated nature of the transport of different species through silica. The activation energies of the permeabilities of water and organic solvents E_i^F are listed in Table 2. Remarkably, the values of $E_{H_2O}^F$ are very close to zero for all three separation processes. This same result was obtained in the pervaporative separation of water from water/isopropanol using microporous silica membranes [19]. The permeability of water in all three separation processes is plotted as a function of temperature in Fig. 3. It appears that F_{H_2O} shows no or only slight thermal activation within experimental error. The values of F_{H_2O} in the 1,4-dioxane and methanol separations are in the same range ($1.5–2.5\times10^{-6}$ $mol\,m^{-2}\,s^{-1}\,Pa^{-1}$), and are close to the measured gas-phase permeability of H_2 (kinetic diameter 2.9 Å) through 400 °C-calcined microporous silica membranes [12]. F_{H_2O} is substantially lower in the process involving DMF.

The molar fluxes of water were 10–200 times larger than the corresponding solvent fluxes in the separations involving 1,4-dioxane and DMF, so that Eq. (10) can be applied to describe F_{H_2O}. And since the activation energy of water permeability $E_{H_2O}^F$ is (close to) zero in both cases, this suggests that water is transported either by gas-phase diffusion, in which case $E_{H_2O}^F = E_{H_2O}^D \approx 0$, or by surface diffusion, in which case $E_{H_2O}^D \approx Q_{H_2O}$.

Water vapor is known to adsorb substantially on microporous silica at moderate temperatures [24,25]. The heat of reversible adsorption of water Q_{H_2O} on crystobalite silica at 30 °C is about 44 kJ/mol [26], and from results of water sorption experiments on microporous silica powders an adsorption coefficient $H_{H_2O} = 3.8\ mol\,m^{-3}\,Pa^{-1}$ at 60 °C can be estimated [24,27]. In view of the small pore size of silica it is not likely that enough space will be left for gaseous diffusion to occur if water adsorption takes place as well. Even without pore narrowing due to adsorbed water molecules the pore diameter is less than two times the molecular diameter of water, so diffusion by gas translation

Table 2
Apparent activation energies of flux (E_{act}) and permeability (E_i^F) in the pervaporation of binary liquids with 15 wt.% water in the feed

Binary liquid	E_{act} (kJ/mol)		E_i^F (kJ/mol)	
	Water	Organic component	Water	Organic component
Water/methanol	47 ± 9	18 ± 17	−4 ± 5	−24 ± 7
Water/dioxane	51 ± 7	9 ± 20	2 ± 6	−29 ± 19
Water/DMF	52 ± 13	13 ± 18	4 ± 9	−35 ± 15

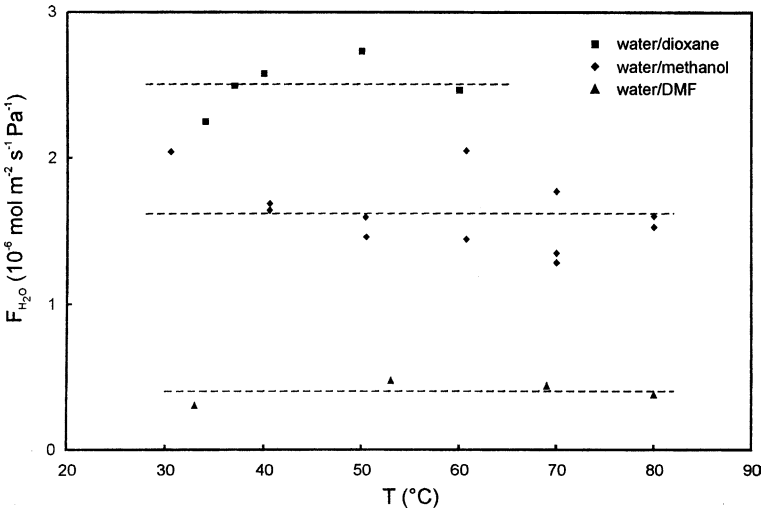

Fig. 3. Permeability of water in pervaporation from 15 wt.% water-containing binary liquids. Broken lines indicate the average permeabilities of water in the respective pervaporation processes.

without any noticeable interaction with the pore walls is not likely.

This strongly suggests that surface diffusion is the main mode of water transport through silica. The activation energy of diffusion $E^D_{H_2O}$ should therefore be in the range of 40–50 kJ/mol. This is a rather high value, considering the fact that water is a small molecule and the activation energies of diffusion of larger non-polar molecules such as H_2, CO_2 (3.3 Å), O_2 (3.45 Å), N_2 (3.6 Å), and CH_4 (3.8 Å) through microporous silica are in the range of 14–30 kJ/mol [12]. In general, the activation energy increases with kinetic diameter for non-polar molecules [12,20]. Possibly, the polar character of water leads to substantial interactions with the pore wall upon diffusion, thereby increasing the activation energy $E^D_{H_2O}$.

In contrast to water, the permeabilities of methanol, 1,4-dioxane and DMF all have negative activation energies. This seems indicative of transport by surface diffusion, since only contributions of adsorption processes to the apparent activation energy can explain net negative values of E^F_i. This implies that the heats of adsorption of all three organic solvents are larger than their respective activation energies of diffusion. No quantitative data are available for the heats of adsorption on silica, except for methanol, for which heats of adsorption of 60 kJ/mol on crystobalite silica [24], and 65 kJ/mol on silicalite-1 [5] have been reported. Adopting the same value for adsorption in microporous silica implies that $E^D_{CH_3OH}$ is roughly in the range of 30–40 kJ/mol.

The molar fluxes of components at 60 °C versus their respective partial pressure differences over the membrane are shown in Fig. 4. The water fluxes in Fig. 4a show a close to linear dependency on the partial pressure difference of water. The water flux in the presence of DMF is substantially smaller than in the presence of 1,4-dioxane or methanol, which illustrates the strong blocking effect that DMF has on the flux of water.

Since the fluxes of 1,4-dioxane and DMF are small compared to the water fluxes and both organic solvents are known to adsorb appreciably on silica [28–30], Eq. (7) can be used to estimate $Đ'_{H_2O,M}$ and the friction coefficients $Đ_{H_2O,dioxane}$ and $Đ_{H_2O,DMF}$ the experimental data of the water/1,4-dioxane and water/DMF separations. In contrast, Eq. (7) is not valid for water/methanol, since the molar fluxes of water and methanol differ only by a factor of 1.5–4, while they adsorb to roughly similar extents [24]. Eq. (7) was therefore fitted only to the water fluxes of the DMF/water and 1,4-dioxane/water data sets, using $H_{H_2O} = 3.8$ mol m^{-3} Pa^{-1} [24]. For the sake of simplicity it was

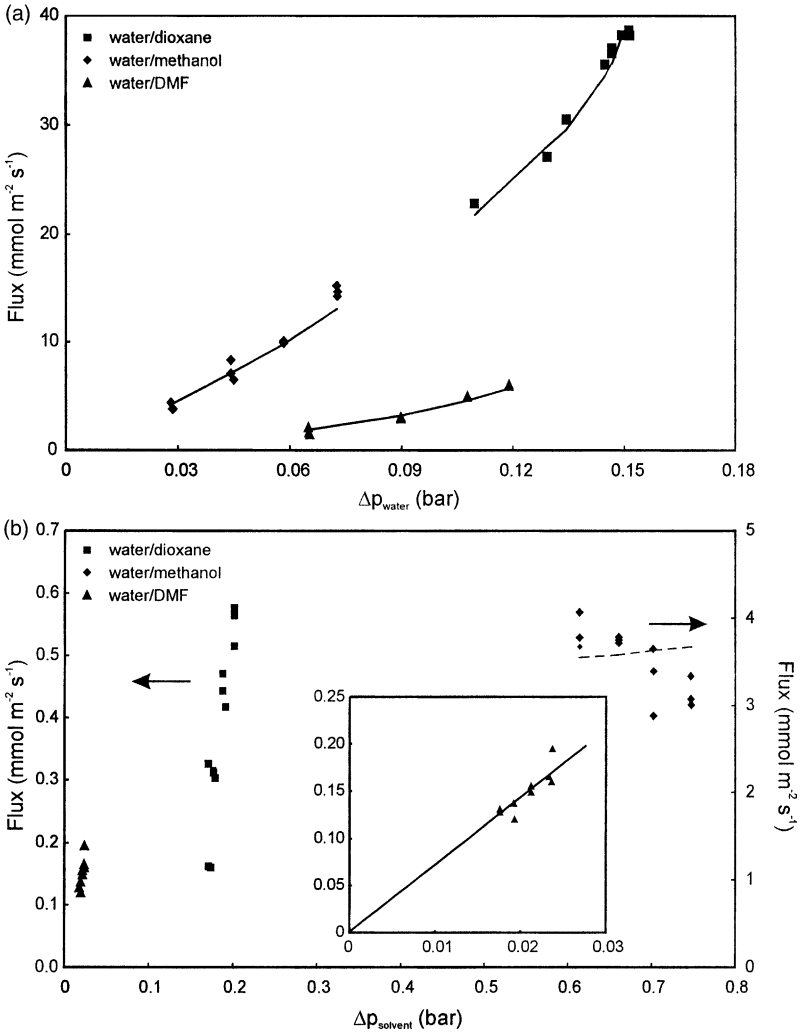

Fig. 4. Dependency of molar flux versus partial vapor pressure difference $\Delta p = p^{f} - p^{p}$ across the membrane at 60 °C: (a) water fluxes and (b) corresponding solvent fluxes. Drawn and broken lines indicate best fits to the Maxwell–Stefan equation (Eq. (4)) and Eq. (7). The inset shows the flux of DMF versus partial pressure difference.

assumed that the friction coefficients have constant values over the entire feed composition interval. Good fits were obtained with the parameters listed in Table 3. In order to estimate the Maxwell–Stefan diffusion coefficients of the methanol/water process, Eq. (4) was fitted numerically to the experimental data. The adsorption coefficient of methanol was assumed to be similar to the adsorption coefficient of water in the calculation, since water and methanol are known to adsorb in similar amounts on silica at the same relative vapor pressure $(p/p^0 = 0.10)$ [24]. The resulting Maxwell–Stefan diffusion coefficients are listed in Table 3 and the fitted curves are shown in Fig. 4.

The water diffusion coefficient $Đ'_{H_2O,M} = 3.1 \times 10^{-13}$ m^2 s^{-1} obtained from the fits is smaller than the value reported by Verkerk et al., who estimated $Đ'_{H_2O,M} = 9 \times 10^{-13}$ m^2 s^{-1} [19]. However, it is noted that H_{H_2O} was assumed to be only 0.8 mol m^{-3} Pa^{-1} in the latter case, which should lead

Table 3
Estimated Maxwell–Stefan micropore diffusion coefficients

Molecule	H_i (mol m^{-3} Pa^{-1})	D_{iM} (m^2 s^{-1})	$D_{i,\mathrm{water}}$ (m^2 s^{-1})
Water	3.8[a]	3.1×10^{-13}	–
Methanol	3.8[b]	2.4×10^{-15}	9.5×10^{-14}
DMF			8.0×10^{-15}
1,4-dioxane			1.1×10^{-13}

[a] Estimated from data in Ref. [24].
[b] Assumed value is adsorption coefficient of water.

to higher predicted values for $Đ'_{H_2O,M}$. The friction coefficients of $Đ'_{H_2O,\mathrm{dioxane}}$ and $Đ_{H_2O,CH_3OH}$ found in this study are $\sim 1\times10^{-13}$ m^2 s^{-1}. This is close to the reported friction coefficient of isopropanol–water $Đ_{H_2O,i\text{–PrOH}} = (0.8\text{–}2)\times10^{-13}$ m^2 s^{-1} [19]. The friction coefficient $Đ_{H_2O,\mathrm{DMF}}$ is more than one order of magnitude smaller.

With respect to $Đ'_{CH_3OH,M}$, only a rough estimate of its magnitude could be obtained. The methanol diffusion coefficient appears to be roughly two orders of magnitude smaller than $Đ'_{H_2O,M}$, but the experimentally observed trend of a methanol flux that decreases with increasing methanol partial pressure difference over the membrane could not be reproduced accurately by the fitted curve, as shown in Fig. 4b. The same trend was observed at low water concentrations in the pervaporation of water/isopropanol with microporous silica–zirconia composite membranes [10]. Fig. 5 shows the same fluxes versus molar composition of the feed. For the methanol/water separation, both the water and methanol flux are seen to increase with molar concentration of water. Qualitatively, this can be understood by rewriting Eq. (4) in the following form:

$$J_s = c_s\left(\frac{x_w}{Đ_{ws}}+\frac{1}{Đ'_{sM}}\right)^{-1}\left[-\frac{1}{p_s}\frac{dp_s}{dz}+\frac{x_w}{Đ_{ws}}\frac{J_w}{c_w}\right], \tag{11}$$

where the indices 'w' and 's' indicate water and second component (methanol), respectively. As can be seen from Eq. (11), the flux of methanol is due to both its own driving force, i.e., the partial pressure gradient dp_s/dz, and a 'dragging' effect that is due to the simultaneous flux of water J_w. To explain the experimentally observed trend in the methanol flux it has to be assumed that the last term containing J_w dominates the first term. An alternative explanation for the observed trend may be that the assumption of linear adsorption (Henry regime) is not valid under the conditions covered by the experiments.

As no accurate quantitative data on the adsorption of DMF and 1,4-dioxane in silica are available, the fluxes of these two compounds could not be fitted quantitatively to Eq. (4). The inset in Fig. 4b illustrates that the DMF flux is roughly proportional to the DMF partial pressure difference. This may imply that dragging by water does not dominate the DMF flux.

In contrast to methanol and DMF, the flux of 1,4-dioxane cannot be explained within the framework of the Maxwell–Stefan theory. Clearly, there is no relationship between the 1,4-dioxane flux and its partial pressure difference over the membrane, but dragging by water does not provide a satisfactory explanation either, since the 1,4-dioxane flux is seen to decrease with increasing J_w. On the other hand, a roughly proportional relationship between the 1,4-dioxane flux and its feed concentration could be observed, as is shown in Fig. 5b. This may imply that 1,4-dioxane permeates through the membrane mainly by transport through larger (meso)pores or small defects in gaseous or liquid-like form. Transport in gaseous form like Knudsen or activated gas-phase diffusion is unlikely, since these mechanisms predict a $1/\sqrt{T}$ temperature dependency for the permeability [20]. This would result in $E^F_{\mathrm{dioxane}} \approx -1.4$ kJ/mol in the temperature interval of 30–80 °C, which does not agree with the value in Table 2. If it is assumed that transport of 1,4-dioxane occurs by viscous flow in liquid-like form, Darcy's law may be applied to describe the (non-selective) flow through these larger pores [31]:

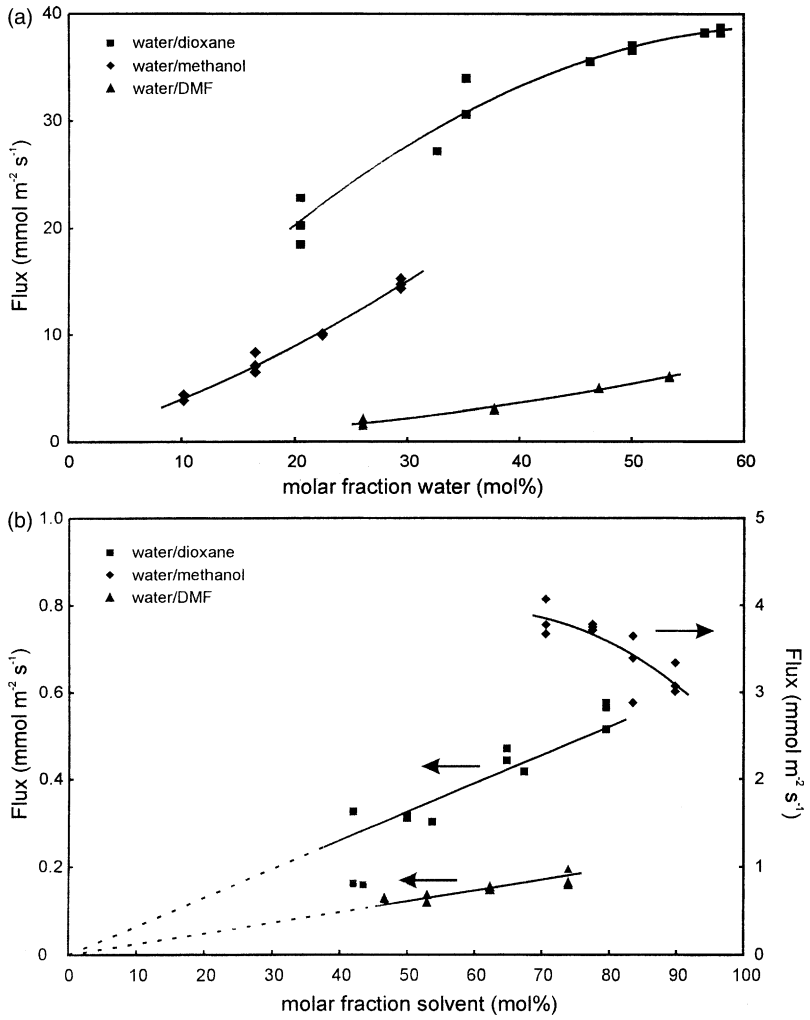

Fig. 5. (a) Water fluxes and (b) corresponding solvent fluxes in pervaporation of binary liquids at 60 °C versus molar composition of retentate. Drawn lines are a guide to the eye.

$$J_v = -\frac{k_m}{\eta}\Delta P. \tag{12}$$

Here J_v is the liquid flux, η the fluid viscosity, ΔP the mechanical pressure difference across the membrane, and k_m the membrane permeability. The latter factor is a structure factor that takes geometrical features of the membrane pores into account (porosity, tortuosity, thickness), so the only thermally activated term in Eq. (12) is the viscosity. For pure 1,4-dioxane and pure water, the inverse viscosities $1/\eta$ increase with temperature with apparent activation energies of 12.5 and 16.4 kJ/mol, respectively [32]. These are reasonably close to the apparent activation energy of the 1,4-dioxane flux (9 ± 20 kJ/mol). Hence, it appears most likely that 1,4-dioxane transport occurs by viscous flow through mesopores or small defects. In view of the fact that the DMF flux is also roughly proportional to its feed concentration (Fig. 5b), it is possible that DMF is also transported partly through mesopores, although the micropore blocking effect exhibited by DMF indicates that it diffuses through micropores as well.

5. Conclusions

Transport of water, methanol and DMF through microporous silica appears to occur by a thermally activated surface diffusion mechanism. The Maxwell–Stefan diffusion coefficients of water and methanol are estimated to be 3.1×10^{-13} and 2.4×10^{-15} $m^2\,s^{-1}$ at 60 °C, respectively. The 1,4-dioxane molecules are probably too large to enter the silica micropores effectively, and they are transported through the silica layer mainly by viscous flow through mesopores or small defects. DMF is thought to adsorb strongly on the internal pore walls, and also because of its large molecular size this causes blocking of micropores. This effect is reflected in the small value of the friction coefficient $Đ_{H_2O,DMF}$, which is more than an order of magnitude smaller than the friction coefficients $Đ_{H_2O,dioxane}$ and $Đ_{H_2O,CH_3OH}$ The flux of methanol at 5–20 wt.% water concentrations in the feed appears to be dominated by a dragging effect by the larger water flux.

Acknowledgements

Financial support of the Commission of the EC in the framework of the Growth Programme, contract no. GIRD-2000-00347 (SUSTOX), is gratefully acknowledged.

References

[1] R.D. Noble, S.A. Stern, in: Membrane Separation Technology: Principles and Applications in Membrane Science and Technology, vol. 2, Elsevier, Amsterdam, 1995.
[2] A. Navajas, R. Mallada, C. Tellez, J. Coronas, M. Menendez, J. Santamaria, Desalination 148 (2002) 25.
[3] S. Li, V.A. Tuan, R.D. Noble, J.L. Falconer, Ind. Eng. Chem. Res. 40 (2001) 4577.
[4] D. Shah, K. Kissick, A. Ghorpade, R. Hannah, D. Bhattacharyya, J. Membr. Sci. 179 (2000) 185.
[5] S. Li, V.A. Tuan, J.L. Falconer, R.D. Noble, Micropor. Mesopor. Mater. 58 (2003) 137.
[6] T. Gallego-Lizon, E. Edwards, G. Lobiundo, L. Freitas dos Santos, J. Membr. Sci. 197 (2002) 309.
[7] H.M. van Veen, Y.C. van Delft, C.W.R. Engelen, P.P.A.C. Pex, Sep. Purif. Technol. 22–23 (2001) 361.
[8] F.P. Cuperus, R.W. van Gemert, J. Membr. Sci. 27 (2002) 225.
[9] J. Sekulić, M.W.J. Luiten, J.E. ten Elshof, N.E. Benes, K. Keizer, Desalination 148 (2002) 19.
[10] M. Asaeda, Y. Sakou, J. Yang, K. Shimasaki, J. Membr. Sci. 209 (2002) 163.
[11] P. Kölsch, M. Sziládi, M. Noack, J. Caro, L. Kotsis, I. Kotsis, I. Sieber, Chem. Eng. Technol. 25 (2002) 357.
[12] R.M. de Vos, H. Verweij, J. Membr. Sci. 143 (1998) 37.
[13] B.N. Nair, K. Keizer, H. Suematsu, Y. Suma, N. Kaneko, S. Ono, T. Okubo, S.-I. Nakao, Langmuir 16 (2000) 4558.
[14] N. Benes, A. Nijmeijer, H. Verweij, in: N.K. Kanellopoulos (Ed.), Recent Advances in Gas Separation by Microporous Ceramic Membranes, Elsevier, Amsterdam, 2000, pp. 335–372.
[15] F. Lipnizki, G. Trägårdh, Sep. Purif. Methods 30 (2001) 49.
[16] A. Heintz, W. Stephan, J. Membr. Sci. 89 (1994) 153.
[17] P. Izák, L. Bartovská, K. Friess, M. Šípek, P. Uchytil, J. Membr. Sci. 214 (2003) 293.
[18] X. Ni, X. Sun, D. Ceng, F. Hua, Polym. Eng. Sci. 41 (2001) 1440.
[19] A.W. Verkerk, P. van Male, M.A.G. Vorstman, J.T.F. Keurentjes, J. Membr. Sci. 193 (2001) 227.
[20] J. Xiao, J. Wei, Chem. Eng. Sci. 47 (1992) 1123.
[21] J. Gmehling, U. Onken, W. Arlt, Vapor–Liquid Equilibrium Data Collection, Dechema, Frankfurt, 1981.
[22] M.E. van Leeuwen, Fluid Phase Equilibr. 99 (1994) 1.
[23] B. van der Bruggen, J. Schaep, D. Wilms, C. Vandecasteele, J. Membr. Sci. 156 (1999) 29.
[24] A.W. Verkerk, Application of Silica Membranes in Separations and Hybrid Reactor Systems, PhD thesis, University of Eindhoven, the Netherlands, 2003, pp. 61–90.
[25] H.E. Wolf, E.-U. Schünder, Chem. Eng. Process. 38 (1999) 211.
[26] V. Bolis, A. Cavenago, B. Fubini, Langmuir 13 (1997) 895.
[27] The adsorption coefficient was estimated from the Langmuir parameters in Table 1 of Ref. [24] according to $H_{H_2O} \approx \rho b q_{sat}$, with $\rho = 1500$ kg/m^3, $b = 2.03 \times 10^{-4}$ Pa^{-1}, and $q_{sat} = 12.67$ kg/mol.
[28] P. Jandera, M. Kučerová, J. Chromat. A 759 (1997) 13.
[29] P. Jandera, L. Petranek, M. Kučerová, J. Chromat. A 791 (1997) 1.
[30] K. Itoh, T. Kimizuka, K. Matsui, Anal. Sci. 17 (2001) i1157.
[31] S.R. Chowdhury, K. Keizer, J.E. ten Elshof, D.H.A. Blank, J. Membr. Sci., in press.
[32] D.R. Lide (Ed.), CRC Handbook of Chemistry and Physics, 75th ed., CRC Press, Boca Raton, 1994.